Integrated Pancreatic Blood Flow: Bidirectional Microcirculation Between Endocrine and Exocrine Pancreas

Michael P. Dybala,[1] Andrey Kuznetsov,[2] Maki Motobu,[2] Bryce K. Hendren-Santiago,[1] Louis H. Philipson,[1,3] Alexander V. Chervonsky,[2] and Manami Hara[1]

Diabetes 2020;69:1439–1450 | https://doi.org/10.2337/db19-1034

The pancreatic islet is a highly vascularized endocrine micro-organ. The unique architecture of rodent islets, a so-called core-mantle arrangement seen in two-dimensional images, led researchers to seek functional implications for islet hormone secretion. Three models of islet blood flow were previously proposed, all based on the assumption that islet microcirculation occurs in an enclosed structure. Recent electrophysiological and molecular biological studies using isolated islets also presumed unidirectional flow. Using intravital analysis of the islet microcirculation in mice, we found that islet capillaries were continuously integrated to those in the exocrine pancreas, which made the islet circulation rather open, not self-contained. Similarly in human islets, the capillary structure was integrated with pancreatic microvasculature in its entirety. Thus, islet microcirculation has no relation to islet cytoarchitecture, which explains its well-known variability throughout species. Furthermore, tracking fluorescent-labeled red blood cells at the endocrine-exocrine interface revealed bidirectional blood flow, with similar variability in blood flow speed in both the intra- and extra-islet vasculature. To date, the endocrine and exocrine pancreas have been studied separately by different fields of investigators. We propose that the open circulation model physically links both endocrine and exocrine parts of the pancreas as a single organ through the integrated vascular network.

Blood flow in the pancreatic islet microcirculation has critical implications for understanding both islet developmental processes and the regulatory islet hormone network. It also has implications for the effect of insulin and other islet hormones on the acinar pancreas or vice versa. The relationship between blood flow patterns and islet cell cytoarchitecture has been the subject of intense debate since the initial descriptions by Orci and Unger (1). Three mutually exclusive models of the direction of islet blood flow have been proposed (2): model 1, from periphery to center of the islet; model 2, from center to periphery; and model 3, from one pole of the islet to the other. Each model was built upon research of an impressive number of articles: 20, 24, and 30 articles published between 1969 and 1995, respectively. Particularly, the unique islet architecture in rodent islets, with endocrine cell types having specific locations within the islet, led to the hypothesis of the functional significance of the hierarchy of endocrine cells in sensing blood glucose levels. The question was whether β-cells or non–β-cells (i.e., α- and δ-cells) should see the initial increments in blood glucose levels. In model 1, afferent blood flows from mantle to core, perfusing non–β-cells first. The direction of the flow is reversed in model 2, in which arterial blood first reaches the β-cells in the core, making the β-cell the primary regulator of islet hormone secretion. Note that both models 1 and 2 exclude paracrine effects of other cell types. Model 3 implies both paracrine and autocrine interactions with a polar pattern of microcirculation regulated by external and internal gates. This model was based on in vivo recording of perfused fluorescent markers that showed a wave across the islet from the afferent to the efferent pole by filling one hemisphere of the islet before flowing across to the other

[1]Department of Medicine, The University of Chicago, Chicago, IL
[2]Department of Pathology, The University of Chicago, Chicago, IL
[3]Department of Pediatrics, The University of Chicago, Chicago, IL

Corresponding author: Manami Hara, mhara@uchicago.edu

Received 11 October 2019 and accepted 9 March 2020

This article contains supplementary material online at https://doi.org/10.2337/db20-4567/suppl.11968926.

See accompanying article, p. 1336.

hemisphere (2,3). Interestingly, models 1 and 2 have been supported by studies using similar techniques, such as scanning electron microscopy of corrosion casts, in vivo microscopy of ink-perfused islets, and tissue staining. Noteworthily, there was an overall agreement that both morphological and intravital evidence at the time may support that all three types of blood circulation could occur (2). Then, over a decade later in 2008, Nyman et al. (4) confirmed the existence of all three patterns of blood flow in live mouse pancreas with different frequency: model 2 (n = 12/20 islets) > model 3 (7/20) > model 1 (1/20). However, the functional significance of having all three patterns of microcirculation was not clear, as the authors stated.

Here, we extensively analyzed the islet blood flow using a large number of in vivo recordings in mice. Islet capillary structure was also examined in thick human pancreas tissue slices. These in vivo and in situ studies contradict the prevailing concept that the islet is an enclosed system that, we hypothesize, is the basis of all three models of islet microcirculation described previously. In fact, the islet has been illustrated as being situated between an afferent arteriole and an efferent venule, indicating the one-way traffic of islet blood flow simply from artery to vein, with no integration to the surrounding exocrine capillary network (5–9). Similarly in in vitro experiments, the islet is assumed to be an enclosed functional unit. Isolated islets lose a substantial amount of endothelial cells through the isolation process and in culture (10–12). Caution needs to be taken when interpreting in vitro experimental results, since isolated islets can behave differently (13).

We propose that the new model of islet microcirculation presented in this study may help develop a better understanding of the regulation of islet hormone secretion, as well as islet formation and development that may dynamically occur in the pancreas as a whole organ. Furthermore, our findings directly relate functional relationships between islets and acinar cells, while the pancreatic endocrine cells have long been defined as contained in encapsulated islets. This model, therefore, has important testable implications for islet hormone interactions both in the islet and in the acinar pancreas, including the concept of islet-acinar communication that may be involved in the pathogenesis of exocrine insufficiency, type 2 diabetes (T2D), and cystic fibrosis–related diabetes (CFRD) (14–16).

RESEARCH DESIGN AND METHODS

Human Pancreas Specimens

Human pancreata were generously provided by the Gift of Hope Organ Procurement Organization in Chicago. Written informed consent from a donor or the next of kin was obtained for use of a sample in research. The use of deidentified human tissues in the study was approved by the institutional review board at The University of Chicago.

Mice

Adult mice (8–15 weeks old) of both sexes on C57BL/6 and NOD background were used. All the procedures involving animals were approved by The University of Chicago Institutional Animal Care and Use Committee.

Intravital Microscopy of the Pancreas

Mice were anesthetized with ketamine (100 mg/kg) (Fort Dodge Animal Health, Fort Dodge, IA) and xylazine (5 mg/kg) (Ben Venue Laboratories, Bedford, OH). After depilation, a pancreas was externalized. To visualize the blood flow, 10^8 RBCs stained with DiI (Thermo Fisher Scientific, Waltham, MA) and/or tetramethylrhodamine (TMRD)-labeled dextran (2,000,000 MW) (Thermo Fisher Scientific) were injected intravenously in the mice just before imaging. Intravital microscopy was conducted using Leica TCS SP5 MP confocal microscope (Leica Microsystems, Mannheim, Germany). Images were recorded and analyzed using Leica LAS-AF as well as Fiji (http://imagej.net/Fiji).

Antibodies

The following primary antibodies were used: mouse monoclonal antipan-endocrine (AB_11157008, HPi1; Thermo Fisher Scientific), rabbit polyclonal anti-CD31 (AB_726362; Abcam), rabbit anti-α smooth muscle actin (α-SMA) (AB_2223021; Abcam), and DAPI (Invitrogen, Carlsbad, CA). The primary antibodies were conjugated with a combination of amine-reactive fluorophores (*N*-hydroxysuccinimide esters; Thermo Fisher Scientific).

Three-Dimensional Pancreas Imaging

A frozen human pancreas tissue block (~5 mm in thickness) was fixed in 4% paraformaldehyde, embedded in 2% agarose gel, and mounted on a vibratome. Sections (600–800 μm in thickness) were collected in cold PBS. These macrosections were then immunohistochemically stained overnight. Optical clearing was carried out by sequential incubation with 20%, 50%, 80%, and 100% (w/v) solutions of D-fructose and 0.3% (v/v) α-thioglycerol (Sigma-Aldrich) for 1–2 h each at 30°C with gentle agitation. A Leica SP8 laser scanning confocal microscope was used to image tissue slices mounted between coverslips. Three-dimensional (3D) reconstruction and analysis were carried out using Fiji and Imaris software (Bitplane, Concord, MA).

Data and Resource Availability

The data sets analyzed in the current study are available from the corresponding author upon reasonable request.

RESULTS

Mouse Islet Architecture

Three previous models of the intraislet blood flow patterns are schematically illustrated in Fig. 1*A*. Detailed descriptions of these models, including experimental methods, observations, interpretations, and functional implications, are summarized in Supplementary Table 1. These models were primarily built upon the cytoarchitecture of laboratory mouse/rat islets, which has been described as a mantle of non–β-cells surrounding a core of β-cells. We reason that two-dimensional views of mouse islets (Fig. 1*B*a and b)

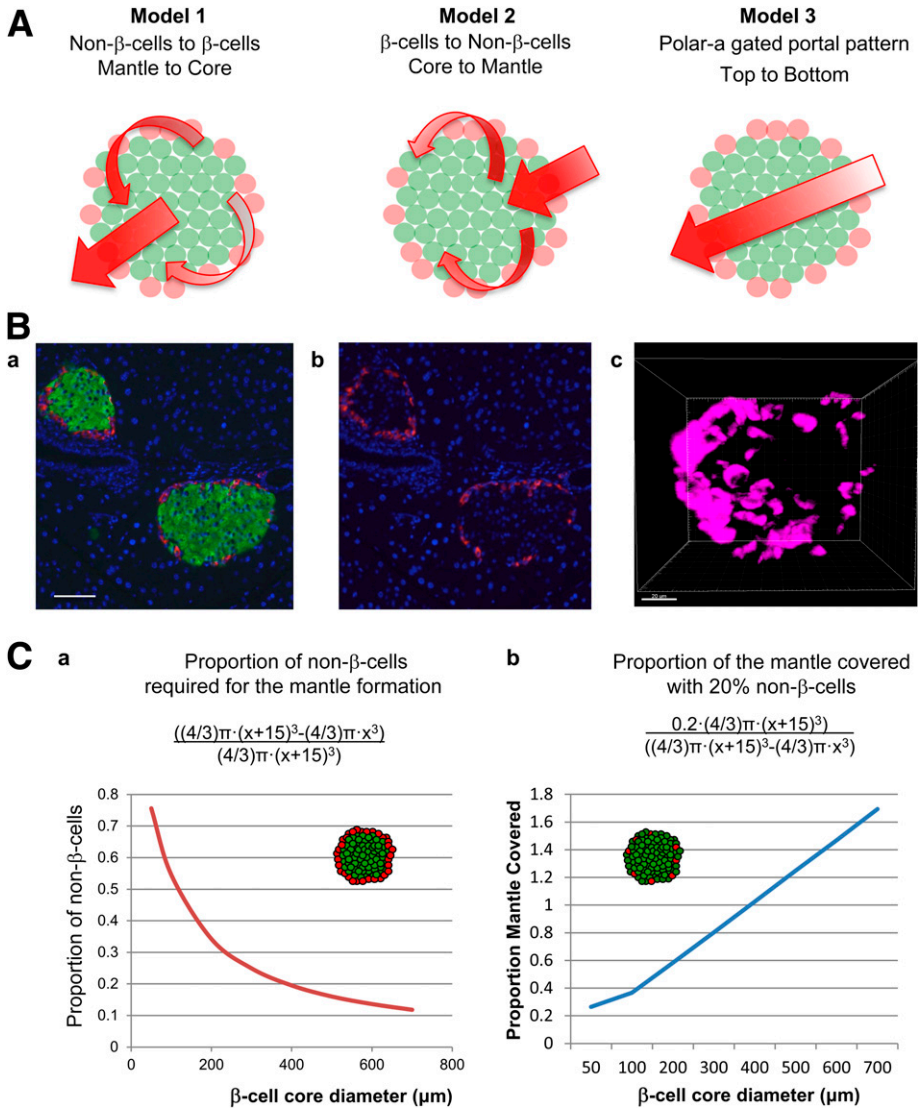

Figure 1—Mouse islet architecture and patterns of microcirculation. *A*: Three models of the direction of islet blood flow. *B*: (a) Two-dimensional image of mouse islets immunostained for insulin (green), glucagon (red), and nuclei (DAPI, blue). Scale bar: 50 μm. (b) α-Cells only. (c) 3D view of α-cell lining. Scale bar: 20 μm. *C*: (a) Proportion of non–β-cells required for the mantle formation. (b) Proportion of the mantle covered with 20% non–β-cells.

may provide an impression that islets have a mantle of non–β-cells and that the islet blood flow is isolated from surrounding exocrine tissue. These images cannot provide an objective assessment of the islet architecture. Thus, we used two different approaches to address this critical methodological limitation.

We examined the possibility of the existence of a complete mantle that would anatomically separate the islet blood supply. In the three-dimensional view, α-cells did not form a complete mantle (17) (Fig. 1*Bc*). Thus, we asked what proportion of non–β-cells would be necessary to form a single-cell layer of a completely enclosed mantle (Fig. 1*C*). It has been previously reported that α- and δ-cells comprise up to 20% of mouse islet endocrine cells (18–23). Mathematical simulation showed that an unrealistic proportion of non–β-cells would be required to cover the β-cell core volumetrically in 3D. The proportion of non–β-cells reaches close to 20%, only when the β-cell core diameter is ~400 μm (Fig. 1*Ca*). Conversely, the proportion of the mantle covered with the 20% of non–β-cells is plotted against the β-cell core diameter (Fig. 1*Cb*). This shows that a small ratio of non–β-cells to total islet cells does not allow formation of a complete mantle within the common range of the islet size distribution, as there are simply not enough cells in the islet to make it.

The Mouse Islet Is Not an Enclosed Micro-Organ

Next, we examined the blood flow in vivo by retro-orbitally injecting mice with fluorescent-labeled red blood cells (RBCs) and recording the flow of RBCs (391 islets from 192 mice), using transgenic mice in which pancreatic β-cells expressed GFP under the control of mouse insulin

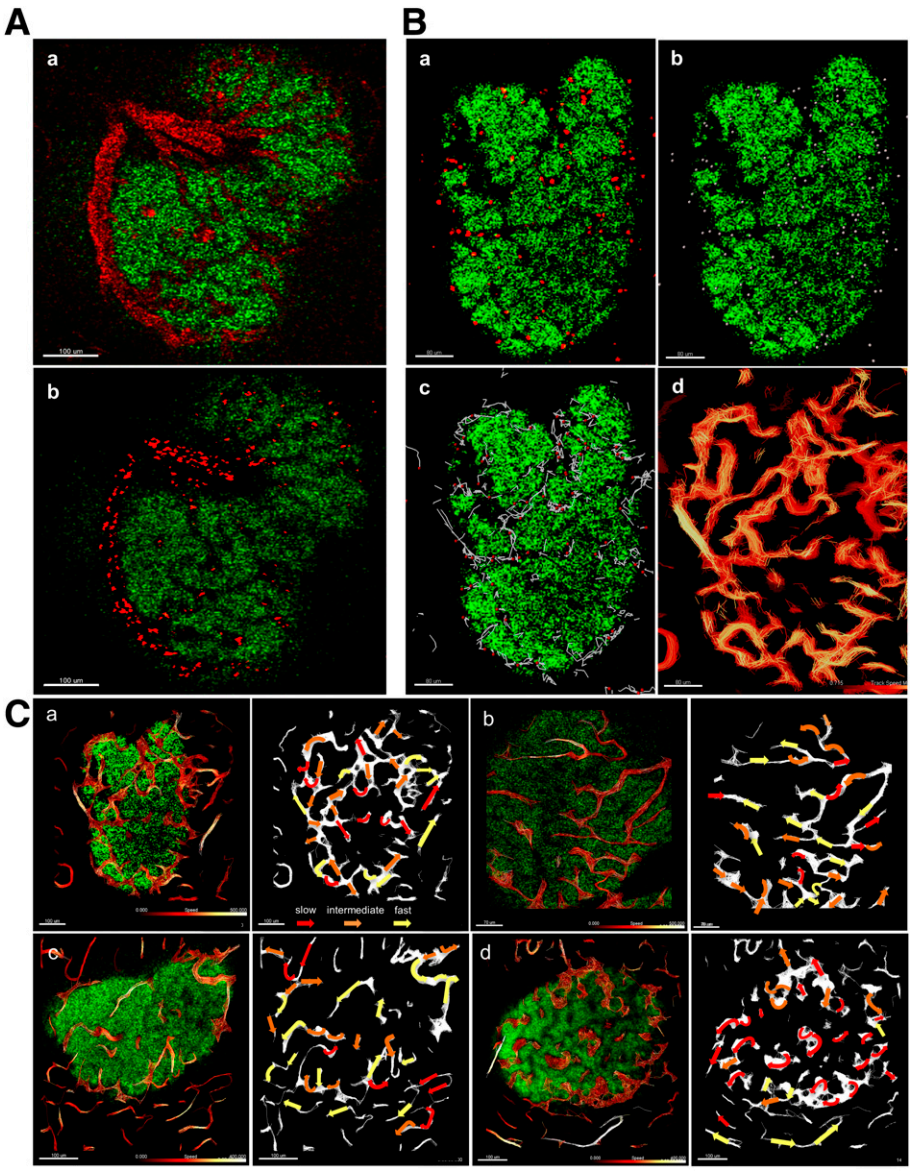

Figure 2—Measurement of RBC flow in mouse islets. *A*: (a) Fluorescent signal of dextran in mouse islet vasculature. (b) Fluorescent signal of labeled individual RBCs in mouse islet vasculature. Scale bar: 100 μm. *B*: (a) Fluorescent signal of labeled individual RBCs. (b) Computer-generated spheres representing tracked RBCs. (c) Computer-generated spheres showing path of RBC movement through tailing. (d) Heatmap of RBC speed within the islet (fast to slow, white to red). Scale bar: 80 μm. *C*: Heatmap of RBC pathways through mouse islets (β-cells in green). (a) (left) Individual pathways are color coded from slow (dark red, 0 μm/s) to fast (white, 500 μm/s). (right) Arrows depict the direction of flow and are color coded according to RBC speed in the indicated region (red, slow; orange, intermediate; yellow, fast). Scale bar: 100 μm. (b) Speed scale 0–500 μm/s. Scale bar: 70 μm. (c) Speed scale 0–400 μm/s. Scale bar: 100 μm. (d) Speed scale 0–400 μm/s. Scale bar: 100 μm. See also Supplementary Videos 1–7.

I promoter (MIP-GFP mice) (24). While a bolus injection of fluorescent-labeled dextran clearly marks the capillary network (Fig. 2*A*a and Supplementary Video 1), only tracking fluorescent-labeled RBCs allowed for exact definition of the direction and speed of flow across intraislet regions (Fig. 2*A*b and Supplementary Video 2). A dextran injection appears as a wave of fluid rapidly perfusing the islet and surrounding tissue (3). In this experiment, we observed fluorescent-labeled RBCs flowing with varying quantities, densities, and speeds within the same islet and among different islets. Furthermore, tracking RBCs enabled us to examine the entire path of the RBCs and determine changes in speed or direction, as they traveled through the islet. In some regions, RBCs exit the islet immediately after entering, whereas in other regions, the RBCs traveled longer paths, while coiling, slowing down, or speeding up, before exiting the islet. This approach allowed us to distinguish the patterns of flow in the capillaries of a single islet as heterogeneous rather than simply unidirectional (e.g., core to periphery, periphery to core, or polar pattern),

and it suggests that islets exist as integrated units within the larger pancreatic vascular network rather than as individual self-contained micro-organs. Fluorescent RBCs flowing through a MIP-GFP islet are shown in Fig. 2*B*a and Supplementary Video 3. Computer-generated representations of individual RBCs (regarded as spheres) were used for enhanced visualization (Fig. 2*B*b and Supplementary Video 4). Supplementary Video 5 shows how individual RBCs are tracked to determine directionality of blood flow (Fig. 2*B*b). They further provide us the overall traces of RBC flow (Fig. 2*B*d and Supplementary Video 6), which demonstrate the great variability in the speed of intraislet blood flow shown via heatmaps indicated from slow (red) to fast (white) (Supplementary Video 7). Diverse islet blood flow patterns are shown in Fig. 2*B*. In the archetypal closed capillary bed such as in mesentery, blood is predicted to generally move unidirectionally, from afferent arterioles to efferent drainage vessels (25). However, intraislet capillaries appeared to be highly connected with their surrounding exocrine tissues, with RBCs following considerably multidirectional, somewhat erratic trajectories.

Bidirectional Blood Flow Between Endocrine (Islet) and Exocrine Pancreas

To further clarify that intraislet circulation is continuous with extra-islet circulation, we first determined the directionality of blood flow by individually tracking each fluorescent-labeled RBC that passed the endocrine-exocrine interface using intravital recordings (Fig. 3*A* and Supplementary Videos 8–11). We then quantified the amount of

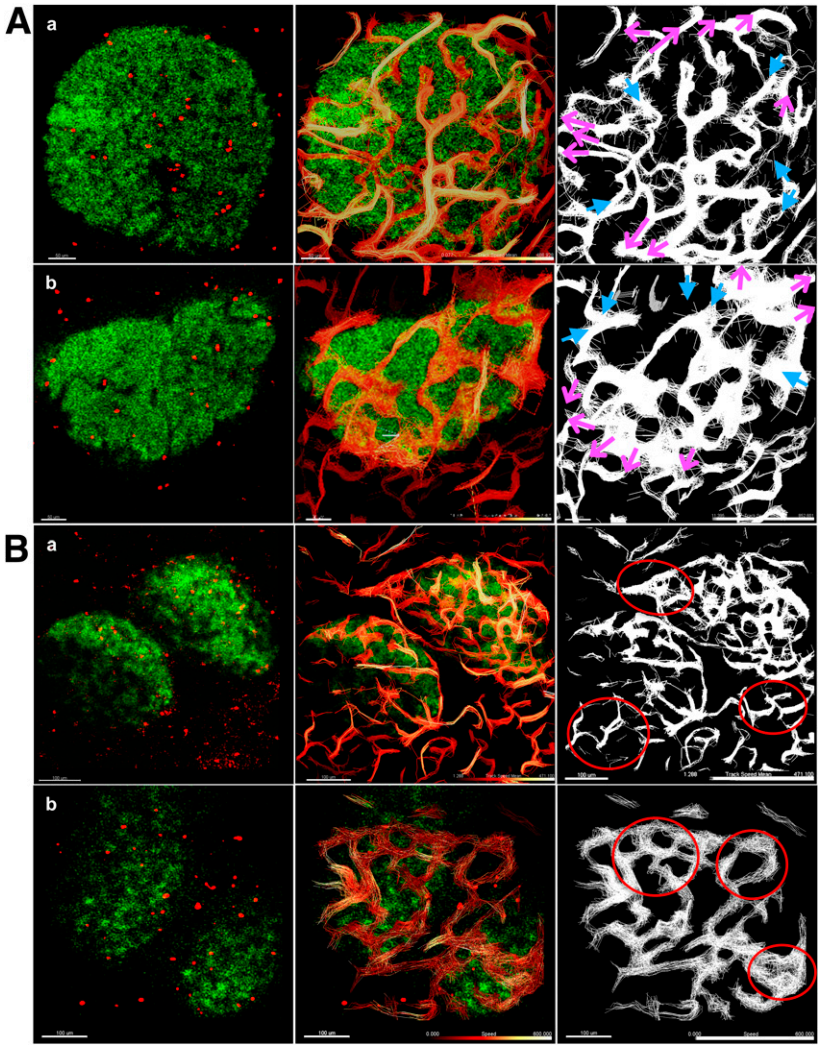

Figure 3— Bidirectional blood flow between endocrine (islet) and exocrine pancreas. *A* (a and b): (left) Fluorescent image of β-cells (green) and RBCs (red). (middle) Fluorescent image of β-cells and heatmap indicating the relative speed of the RBC flow from slow (red) to fast (white). (right) Blood flow direction at the endocrine-exocrine interface was determined by tracking each fluorescently labeled RBC. Exocrine to endocrine (blue arrows). Endocrine to exocrine (pink arrows). Scale bar: (a) 50 μm; (b) 80 μm. *B* (a and b): (left) Fluorescent image of β-cells (green) and RBCs (red). (middle) Fluorescent image of β-cells and heatmap of the relative speed of the RBC flow. (right) Similarly varied flow speed in intra- and extra-islet area was noted (red circles). Scale bar (a and b): 100 μm. See also Supplementary Videos 8–15.

blood vessels that indicated the direction of blood flow between endocrine (islet) and exocrine pancreas at the interface. Blood flow direction from exocrine to endocrine was marked by a blue arrow and that from endocrine to exocrine was marked by a pink arrow (Fig. 3*A*, right). The ratio of the two directions was *1*) exocrine to endocrine: 50.1% ± 1.3% and *2*) endocrine to exocrine: 49.9% ± 1.3% (n = 42 islets). This result serves to validate the notion of bidirectional blood flow rather than unidirectional blood flow as previously reported (5–9). In addition, we hypothesized that this integration of blood flow in its entirety may contradict the prevalent model that islet blood flow is 5- to 10-fold higher compared with the exocrine pancreas (9,26). Indeed, heatmaps of mean speed of RBC flow shown in Fig. 3*B* demonstrates that flow speed varies similarly in both intra- and extra-islet area (Supplementary Videos 12–15).

Mouse Islet Capillaries Are Integrated in the Pancreatic Vascular Network

The structural relationship between islets and capillary networks was examined by retro-orbitally injecting TMRD-labeled dextran to MIP-GFP mice. Z-stack images were captured using a two-photon confocal microscope, which detected fluorescent signals up to 100 μm in depth. This imaging and 3D rendering enabled us to visualize an outer

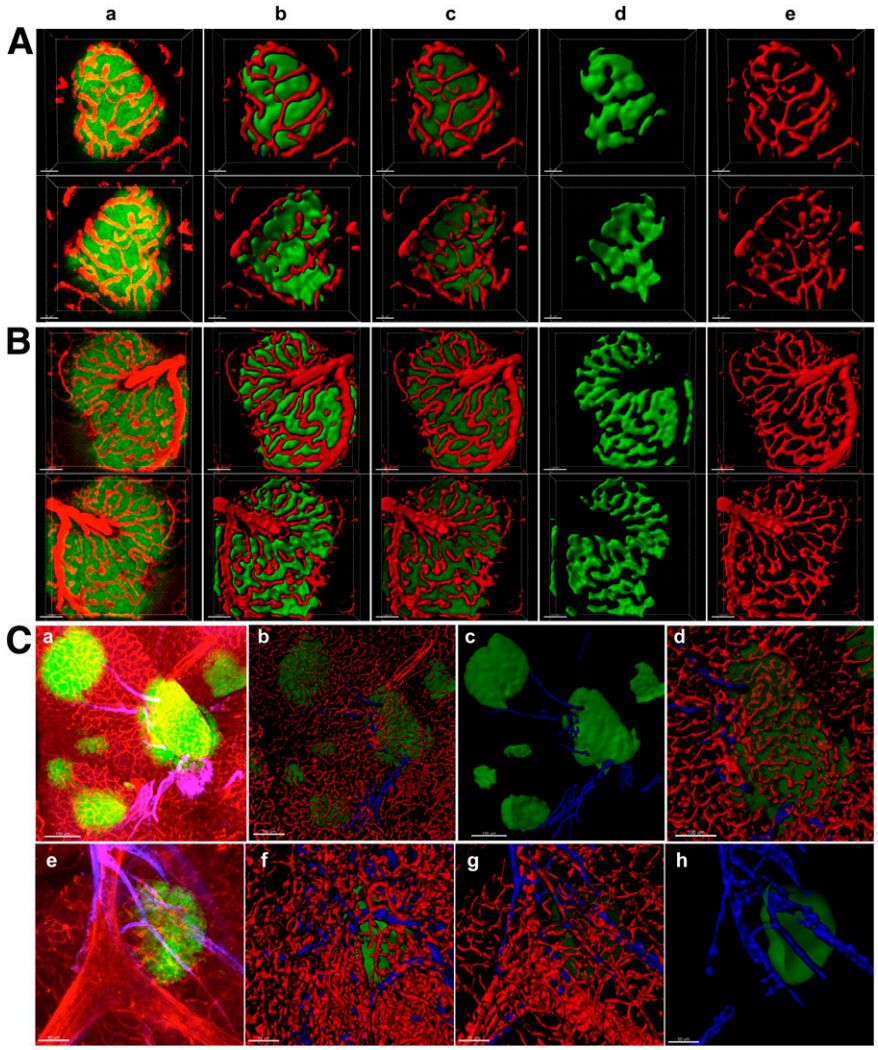

Figure 4—Structural relationship between islets and capillary networks in mouse islets. *A*: Outer layer (upper row) and inner layer (lower row) views of mouse islet (β-cells in green and blood vessels in red). Islet capillaries were noted to be integrated with those in the exocrine tissue. This pattern was observed in islets of different size ranges. Feret's diameter: 314 μm. Scale bar: 50 μm. (a) Fluorescent signals. (b) 3D-rendered β-cells and blood vessels. (c) β-Cells made transparent. (d) β-Cells. (e) Blood vessels. *B*: Feret's diameter: 644 μm. Scale bar: 100 μm. *C*: 3D analysis of mouse islets. (Upper row) (a) Fluorescent image. β-Cells (GFP in green), blood vessels (tomato-lectin in red), and large blood vessels and arterioles (α-SMA in magenta). (b) 3D-rendered image of (a). (c) Blood vessels removed. (d) Islet enlarged and β-cells made transparent. Scale bar: 150 μm for (a–c) and 100 μm for (d). (Lower row) (e) Fluorescent image. (f) 3D-rendered β-cells, blood vessels, and arterioles. (g) 3D-rendered and clipped in half. β-Cells made transparent. (h) Blood vessels removed, β-cells made transparent, and surfaces clipped in half. Scale bar: all 50 μm.

layer (upper rows) and an inner layer (lower rows) of an islet (Fig. 4*A* and *B*). Capillary networks appeared to be continuously integrated inside and outside of the islets, which were naturally denser in larger islets (27). The 3D image analysis of mouse islets showed afferent arterioles feeding into an islet, shown by α-SMA staining in blue (Fig. 4*C*), as we have previously reported in human pancreatic tissue specimens (27). By constructing 3D images of the islet cells and vasculature that constitute the endocrine pancreas, the blood vessels within the islet microenvironment were shown to continuously traverse through both the endocrine and exocrine tissue. Additionally, observation of an afferent arteriole feeding into an islet suggests that this vasculature framework is structurally conserved across mouse and human pancreata.

Human Islet Capillaries Are Also Integrated in the Pancreatic Vascular Network

To examine whether similar capillary integration would be observed in the human pancreas, freshly frozen pancreatic tissue blocks from several organ donors were used for 3D imaging. Human islets from these donor pancreata are shown in Fig. 5. The integration between islet capillaries and those in the exocrine pancreas was similar in mice and humans. Islets, or endocrine cell mass, were shown to be literally embedded in the pancreatic vascular network (Fig. 5*A*a and b and Supplementary Video 16). The predominant pattern was that one arteriole fed an islet indicated by α-SMA staining in yellow (Fig. 5*A*a–m), being consistent with our previous report (27). The pancreatic vascular network was observed to be entirely continuous, not disrupted by islets (Fig. 5*A*a–c, i–l, n, and o). Such capillary integration was confirmed in multiple human pancreata, as shown in Fig. 5*B–D*. In a cluster of islets, some islets were as close as the width of only a single capillary (Fig. 5*E*). Construction of 3D images of the human islet microenvironment supports the idea of a completely integrated pancreatic vascular network. The observation of islets that are separated by the width of a single capillary provides support that there is not a physical barrier that completely isolates the islets from the adjacent exocrine tissue.

Characteristics of Pancreatic Capillary Networks in Patients With T2D

Further structural analysis of the vascular network in patients with T2D revealed integrated exocrine and endocrine capillaries within the pancreas. Islets from a patient with T2D (59-year-old female, duration 15 years) appeared to cluster together in specific regions of the exocrine tissue in more densely vascularized areas (Fig. 6*A*a and b). By constructing 3D surface renditions of the pancreatic islets and vasculature, structurally intact blood vessels were observed demonstrating complete continuity between both endocrine and exocrine tissue blood vessels (Fig. 6*B*a–c). Other cases of T2D are shown in Supplementary Fig. 1. There was no change in the number of arteriole input per islet associated with T2D. While this integration of capillary networks was retained in patients with T2D, morphological changes of capillaries may occur (Fig. 6*C*a–d; a 44-year-old female, duration 15 years), compared with those in a nondiabetic subject (a 46-year-old female; Fig. 6*C*e–h).

Summary

Beyond the debate over the previous three models of islet microcirculation, we demonstrated that the islets in both mice and humans are not enclosed, glomerulus-like structures but rather open ones in which islet capillaries are continuously integrated with those in the exocrine pancreas (Fig. 7). The old model of islet microcirculation and the new integrated model that we propose in the current study are schematically illustrated in Fig. 7*A*. Here, we further verified this capillary integration in its entirety by generating a 3D print based on a stack of single-channel imaging of CD31 signals (Fig. 7*B*a, left). A 3D print on the right highlights the intraislet capillaries in orange, which was generated by cropping the intraislet capillaries out of the whole capillary network based on the HPi1 staining (i.e., a pan-endocrine cell marker). Thus, combining two separate 3D-reconstructed image files (one for the intraislet capillaries in orange and another for the surrounding exocrine capillaries in clear color), the intraislet capillaries were visualized. Figure 7*B*b shows the opposite side of two 3D prints. We reason that if there is no complete integration of the vasculature network in the pancreas as a single organ, such physical 3D printing should not have been accomplished solely based on single channel signals of CD31 staining. Further 3D prints with coloration illustrate the integration of the islet capillary bed in the greater pancreatic vascular network (Fig. 7*C–E*). Physical 3D visualization allows for appreciation of the complexity of islet circulation.

DISCUSSION

In the current study, we first addressed the decades-long controversy of islet microcirculation from several aspects. *1*) There is no complete mantle formation in mouse islets, which was deduced from two-dimensional imaging, but not found in 3D imaging (17,22). *2*) The striking plasticity of islet architecture throughout species (28) calls into question the feasibility of modeling islet blood flow exclusively on rodent islet cytoarchitecture. In fact, studies reported in Brunicardi et al. (2) included numerous species besides rat and mouse, such as rabbit, guinea pig, cow, horse, monkey, and human. However, the differences among the islet blood flow in these species, suggesting a high degree of architectural islet plasticity, were not further incorporated into a universal model. *3*) It appears that isolated blood circulation within an islet was presumed in all three models. This assumption might have provided an ultimate basis for developing the models in the first place. Our analysis of in vivo mouse islet blood flow recordings demonstrated that islet microcirculation is not isolated from the microenvironment, but that many capillary

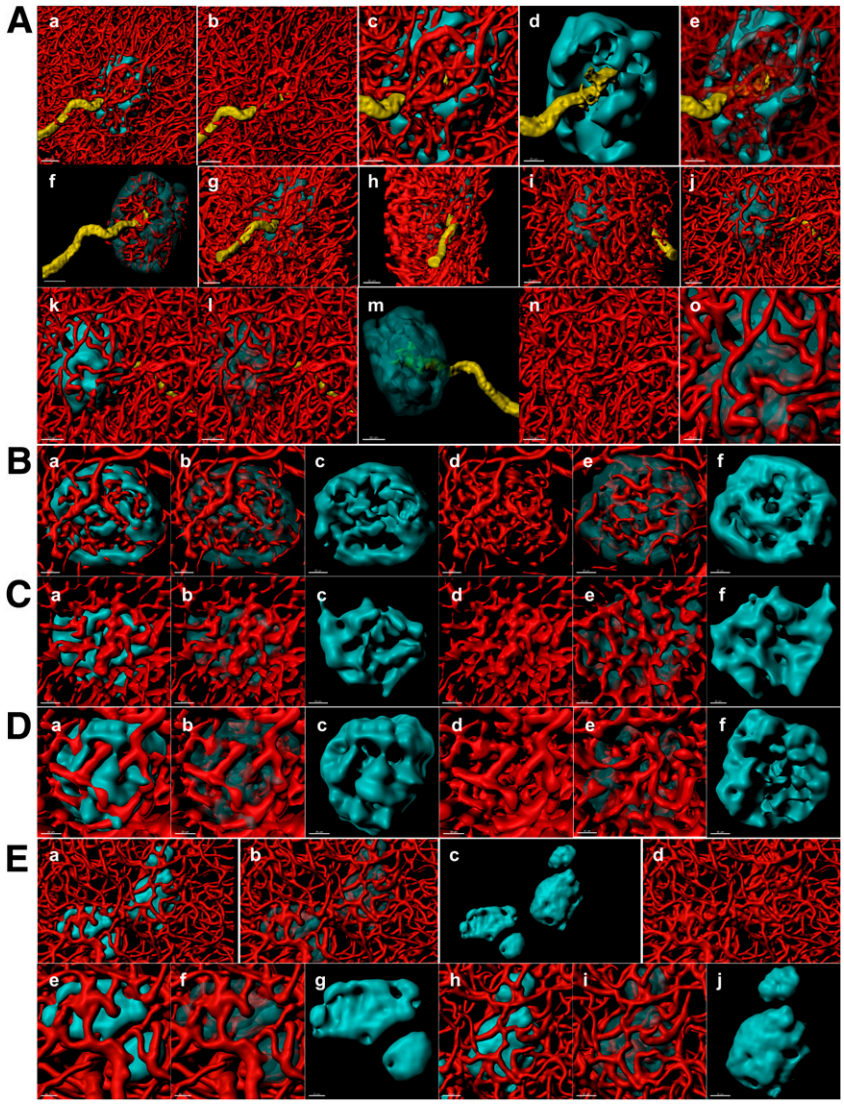

Figure 5— Integrated islet capillaries with those in the exocrine pancreas in human islets. *A*: 3D analysis of a human islet from a 24-year-old male. (a) A 3D-rendered view of a human islet integrated in the pancreatic capillary network. Islet (HPi1, a human pan-endocrine cell marker in cyan), blood vessels (CD31 in red), and an afferent arteriole (α-SMA in yellow). Scale bar: 50 μm. (b) Blood vessels only, displaying the continuity of capillaries in the islet as well as exocrine tissue. (c) Close-up view of (a), with capillaries showing diverse routes of blood flow around the islet and one large afferent arteriole (yellow). Scale bar: 30 μm. (d) The aforementioned feeding arteriole penetrating the center of the islet. (e) Vasculature partially made transparent. (f) Islet made partially transparent without surrounding capillaries. The diverse routes of blood flow observed here within the islet contradict previous models of islet microcirculation. Scale bar: 50 μm. (g–j) Anticlockwise front to back rotation of the islet. The islet is embedded in the larger pancreatic vascular network. Scale bar: 50 μm. (k) Back view. (l) Islet made transparent. (m) Islet made transparent without capillaries, with feeding arteriole penetrating deep into the center of the islet. (n) Capillaries only. Note the continuity of the capillaries regardless of the islet border. (o) Close-up view of the interface of capillaries entering and exiting the islet. Scale bar: 20 μm. *B*: (a) Islet from a 46-year-old female. (b) Islet made transparent. (c) β-Cells only showing openings for capillary entry/exit. (d) Capillaries only. (e and f) Back view. Scale bar: 30 μm. *C*: Islet from a 57-year-old male. Scale bar: (a–c) 40 μm; (d–f) 30 μm. *D*: Islet from a 16-year-old female. Scale bar: 30 μm. *E*: (a) A cluster of four islets from a 24-year-old male. (b) Islet made transparent. (c) Islets. (d) Capillaries. Scale bar: 50 μm. (e–g) Islets in the lower left. Scale bar: 20 μm. (h–j). Islets in the upper left. Scale bar: 30 μm. See also Supplementary Video 16.

branches exit an islet before circulating through the entire structure. Such blood flows were made clearly visible by labeling individual RBCs. Quantitative examination of the amount of blood vessels going in or out of endocrine pancreas (islet) at the interface plainly demonstrated the 1:1 ratio, indicating the integrated capillary network in its entirety. Furthermore, similar variability in the RBC flow speed in both intra- and extra-islet area confirmed that islet blood perfusion is not regulated independently from that of the exocrine pancreas. There is no 5- to 10-fold difference in the RBC flow. The concept of an enclosed system may have originated from comparing the islet capillary network to blood flow in the renal glomerulus (2,5,8), and therefore, further functional resemblance may have

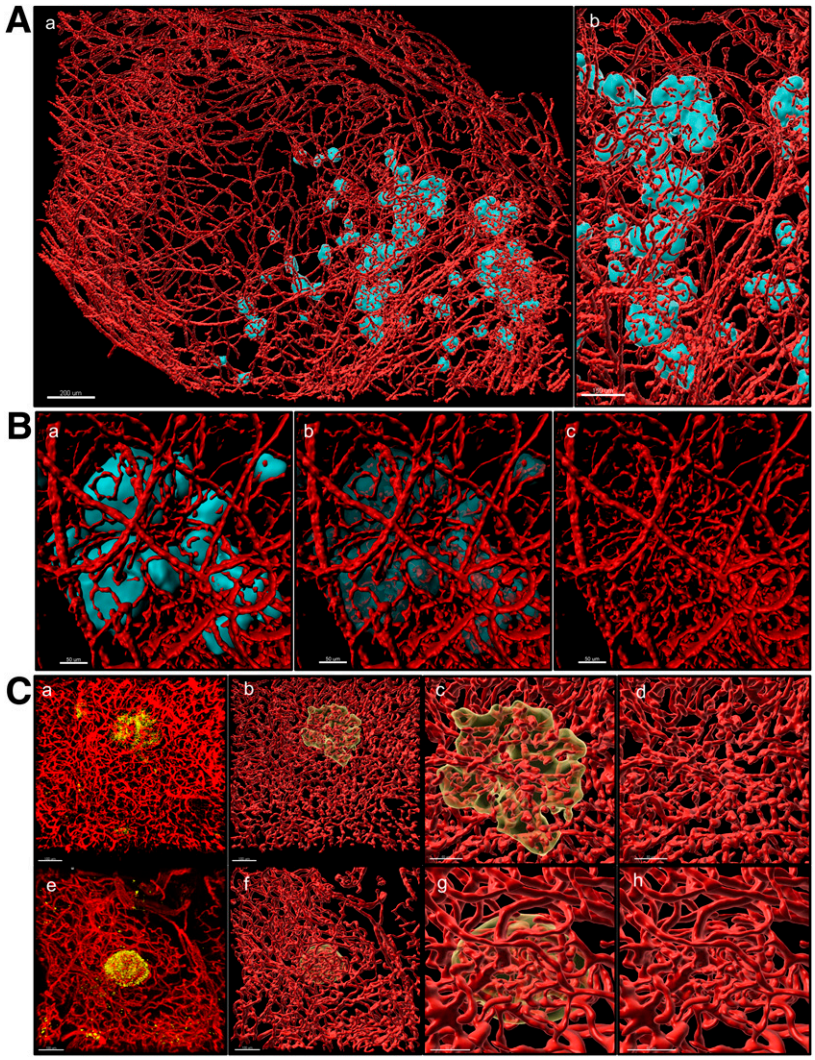

Figure 6—Characteristics of pancreatic capillary networks in patients with T2D. *A*: (a) Large-scale capture of the pancreas in a patient with T2D exhibiting clustered islets (59-year-old female, T2D duration for 15 years; HPi1, a pan-endocrine cell marker in cyan; blood vessels (CD31 in red). Scale bar: 200 μm. (b) Enlarged view of (a). Scale bar: 150 μm. *B*: (a) Clustered islets. (b) Islets made transparent. (c) Blood vessels only demonstrating continuity between endocrine and exocrine vasculature. Scale bar: all 50 μm. *C*: Comparison between a nondiabetic subject and a patient with T2D. (a) A 44-year-old female patient with T2D. Fluorescent image of islet (HPi1 in yellow) and blood vessels (CD31 in red). Scale bar: 100 μm. (b) 3D rendering of (a). Scale bar: 100 μm. (c) Enlarged view of the islet and surrounding blood vessels. Scale bar: 50 μm. (d) Blood vessels only, showing continuity between endocrine and exocrine vasculature. Scale bar: 50 μm. (e–h) The same as (a–d) but for a nondiabetic 46-year-old female. See also Supplementary Fig. 1.

been presumed as well. However, the glomerular capillary bed differs distinctively from that of the islet, both structurally and functionally. The glomerulus is a tuft of capillaries confined between two arterioles of different sizes, with a wider afferent arteriole and a narrower efferent arteriole that maintain high blood pressure in the glomerular capillaries (29). The glomerulus is not considered a functional unit but is instead viewed as a component of the renal corpuscle together with the Bowman's capsule (the blood-filtering component of the nephron of the kidney). This renal corpuscle and the renal tubule comprise the nephron, which is the basic filtration unit of the kidney.

The current study highlights the open nature of microcirculation through the islet. Isolated islets, removed from their integrated capillary network, may therefore behave quite differently from islets in vivo. Caution needs to be taken in studies using isolated islets, as well as in single-cell studies that are prepared by further digesting isolated islets into single-cell suspension followed by FACS sorting. It is well known that during culture, a considerable loss of intraislet blood vessels occurs (10–12). As the islet is a highly vascularized structure, significant alterations may occur following these enzymatic and mechanical treatments, not only in the islet cytoarchitecture but also, plausibly, in the hormone interaction web and gene expression. These possible intermediate changes have never been systematically studied, but they have basically been ignored in the past studies. As an extreme example, dissociated single

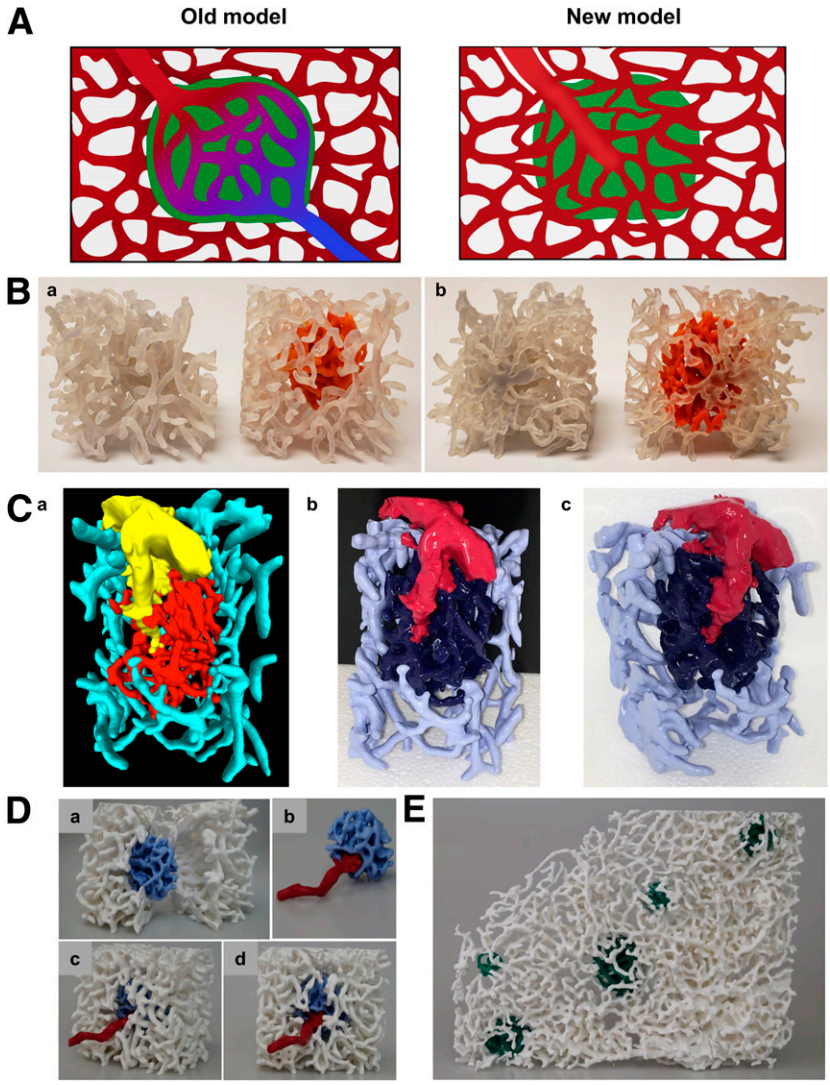

Figure 7—Summary of findings. *A*: (left) Old model of islet (green) microcirculation represented as an isolated system with an afferent arteriole (red) branching into a capillary network and exiting through an efferent venule (blue). (right) New model showing open circulation where an afferent arteriole enters into the islet (green) and branches out into a capillary network integrated with the microenvironment. *B*: 3D prints of a human islet. (a) Side-by-side comparison of the same region of pancreas with exocrine and endocrine (intraislet) capillaries printed the same color (left, clear) and the exocrine capillaries in clear and endocrine capillaries in orange (right). (b) Another view of the same region of pancreas with exocrine and endocrine capillaries in clear (left) and endocrine capillaries in orange and exocrine capillaries in clear (right). *C*: 3D prints with coloration. (a) The computer-generated model from fluorescent 3D imaging used to create the 3D prints in (b) and (c). (b) Front view of a 3D-printed islet and exocrine vasculature. Note the many connections between the endocrine and exocrine vasculature at the islet border. (c) Side view of 3D-printed islet vasculature with a feeding arteriole (red) penetrating the center of the islet. Capillaries within the islet (dark blue) are integrated with vasculature in the exocrine tissue (light blue). *D*: A more expansive view of the endocrine/exocrine vascular network with feeding arteriole shown in *C*. Blood vessels within the islet (light blue) are integrated with those in the exocrine tissue (white). A feeding arteriole (red) penetrates the center of the islet. (a) A cross-sectional view of the islet capillary network within the exocrine tissue vasculature. (b) Islet capillaries with a feeding arteriole. Note the markedly larger size of the feeding arteriole compared with endocrine blood vessels. (c) Side view of the endocrine and exocrine vascular network. (d) Front view of the endocrine and exocrine vascular network. *E*: Human islet vascular network embedded in the exocrine vasculature. Blood vessels in five human islets (dark green) integrated with the pancreatic vascular network (white).

islet cells can reaggregate in vitro (30,31), which was the basis of the previous epithelial-to-mesenchymal transition cell aggregation model (32–36), together with the presence of singly scattered endocrine cells observed throughout the pancreas. However, Sharon et al. (13) recently proposed a new model of islet formation as budding in cohesion based on an in vivo analysis.

The bidirectional open islet circulation may provide mechanistic implications, at least in part, regarding: *1*) The recent intriguing observations that pancreas size is decreased in young children with type 1 diabetes (37,38). Since the acinar tissue would see higher concentrations of insulin than the rest of the body in this integrated blood circulation model, a lack of insulin in children with type

1 diabetes, as a growth factor for the acinar cell (39–42), may result in a smaller pancreas and subsequently deteriorated exocrine function compared with control subjects. *2*) The β-cell hub model, in which a small population of leader/pacemaker β-cells are highly connected to other follower β-cells (43–45). In glucose-stimulatory conditions, these hubs temporally appear in the periphery of an islet, which may control pulsatile insulin secretion. This arrangement may fit better in our integrated open circulation model than in an enclosed circulation, since the leader β-cells in the periphery of an islet should sense blood glucose levels first, all around at the same time, similarly to their experimental settings. *3*) Islet formation and development. Islets are formed within the exocrine pancreas in vivo, not anywhere else, as demonstrated by Krapp et al. (46). In pancreas transcription factor 1-p48 null mice lacking the exocrine pancreas, spared pancreatic endocrine cells were found in the spleen and were individually scattered without forming islets. Integration of islet capillaries and those in the surrounding exocrine tissues may reflect how islets develop together with the vasculature. However, transplanted mature islets may survive outside of the pancreas, such as in liver or under kidney capsule, since vascular endothelial growth factor-A signaling is only necessary during development but not in adult islets (47). *4*) Functional relationship between islets and acinar cells. Unlike other endocrine organs, only in the pancreas, numerous microscopic islets are embedded in the primarily exocrine gland of the pancreas. The concept of islet-acinar axis proposes an essential role of the endocrine and exocrine parts of the pancreas that islet hormones and associated humoral factors regulate the exocrine function (14,15). *5*) The bidirectional blood flow may also enhance our understanding regarding CFRD. When β-cells only minimally express the cystic fibrosis transmembrane conductance regulator (0.45%) (16), the bidirectional blood flow may better support the β-cell extrinsic hypothesis for CFRD over the β-cell intrinsic hypothesis, since exocrine-derived factors such as IL-6 can directly affect β-cell/islet function.

The endocrine pancreas (islets) and the exocrine pancreas have mostly been studied separately. Here, we propose that the open circulation model physically links both parts of the pancreas as a single organ through the integrated vascular network. This new paradigm may provide revived or contrasting insights into the findings of past studies, as well as a novel approach for prospective research projects. Future studies should include the neuronal network within the pancreas, which may shed light on how humoral secretion is regulated by the dynamic interaction of endocrine, paracrine, and neurocrine signals that are closely associated with blood flow.

Acknowledgments. The authors thank Piotr Witkowski and J. Michael Millis at The University of Chicago, and Martin Jendrisak and the entire team of the Gift of Hope Organ and Tissue Donor Network in Chicago, IL, for providing the human pancreas tissues used in the current study.

Funding. The study is supported by National Institutes of Health National Institute of Diabetes and Digestive and Kidney Diseases grants, DK-117192 and DK-020595, to The University of Chicago Diabetes Research and Training Center (Physiology Core), and a gift from the Kovler Family Foundation to M.H. Imaging was performed at The University of Chicago Integrated Light Microscopy Facility. The 3D printing was carried out at the Material Research Science and Engineering Center Shared User Facilities (National Science Foundation DMR-1420709).

Duality of Interest. No potential conflicts of interest relevant to this article were reported.

Author Contributions. M.P.D., B.K.H.-S., and M.H. performed 3D human and mouse pancreas tissue studies, analyzed data, and wrote the manuscript. M.P.D., B.K.H.-S., L.H.P., A.V.C., and M.H. discussed and edited the manuscript. A.K., M.M., L.H.P., and A.V.C. performed mouse in vivo studies. M.H. conceived the idea and designed the study. M.H. is the guarantor of this work and, as such, had full access to all the data in the study and takes responsibility for the integrity of the data and the accuracy of the data analysis.

Prior Presentation. Data in this article were presented at Imaging the Pancreas in Diabetes, and Benign and Malignant Exocrine Pancreatic Disease, National Institute of Diabetes and Digestive and Kidney Diseases, Bethesda, MD, 13–14 January 2020.

References

1. Orci L, Unger RH. Functional subdivision of islets of Langerhans and possible role of D cells. Lancet 1975;2:1243–1244

2. Brunicardi FC, Stagner J, Bonner-Weir S, et al.; Long Beach Veterans Administration Regional Medical Education Center Symposium. Microcirculation of the islets of Langerhans. Diabetes 1996;45:385–392

3. McCuskey RS, Chapman TM. Microscopy of the living pancreas in situ. Am J Anat 1969;126:395–407

4. Nyman LR, Wells KS, Head WS, et al. Real-time, multidimensional in vivo imaging used to investigate blood flow in mouse pancreatic islets. J Clin Invest 2008;118:3790–3797

5. Bonner-Weir S, Orci L. New perspectives on the microvasculature of the islets of Langerhans in the rat. Diabetes 1982;31:883–889

6. Eberhard D, Kragl M, Lammert E. 'Giving and taking': endothelial and beta-cells in the islets of Langerhans. Trends Endocrinol Metab 2010;21:457–463

7. Cleaver O, Dor Y. Vascular instruction of pancreas development. Development 2012;139:2833–2843

8. Pénicaud L. Autonomic nervous system and pancreatic islet blood flow. Biochimie 2017;143:29–32

9. Jansson L, Carlsson PO. Pancreatic blood flow with special emphasis on blood perfusion of the islets of Langerhans. Compr Physiol 2019;9:799–837

10. Parr EL, Bowen KM, Lafferty KJ. Cellular changes in cultured mouse thyroid glands and islets of Langerhans. Transplantation 1980;30:135–141

11. Nyqvist D, Köhler M, Wahlstedt H, Berggren PO. Donor islet endothelial cells participate in formation of functional vessels within pancreatic islet grafts. Diabetes 2005;54:2287–2293

12. Olsson R, Maxhuni A, Carlsson PO. Revascularization of transplanted pancreatic islets following culture with stimulators of angiogenesis. Transplantation 2006;82:340–347

13. Sharon N, Chawla R, Mueller J, et al. A peninsular structure coordinates asynchronous differentiation with morphogenesis to generate pancreatic islets. Cell 2019;176:790–804

14. Barreto SG, Carati CJ, Toouli J, Saccone GT. The islet-acinar axis of the pancreas: more than just insulin. Am J Physiol Gastrointest Liver Physiol 2010;299:G10–G22

15. Pierzynowski SG, Gregory PC, Filip R, Woliński J, Pierzynowska KG. Glucose homeostasis dependency on acini-islet-acinar (AIA) axis communication: a new possible pathophysiological hypothesis regarding diabetes mellitus. Nutr Diabetes 2018;8:55

16. White MG, Maheshwari RR, Anderson SJ, et al. In situ analysis reveals that CFTR is expressed in only a small minority of β-cells in normal adult human pancreas. J Clin Endocrinol Metab 2020;105:1366–1374

17. Dybala MP, Hara M. Heterogeneity of the human pancreatic islet. Diabetes 2019;68:1230–1239
18. Brelje TC, Scharp DW, Sorenson RL. Three-dimensional imaging of intact isolated islets of Langerhans with confocal microscopy. Diabetes 1989;38:808–814
19. Brissova M, Fowler MJ, Nicholson WE, et al. Assessment of human pancreatic islet architecture and composition by laser scanning confocal microscopy. J Histochem Cytochem 2005;53:1087–1097
20. Cabrera O, Berman DM, Kenyon NS, Ricordi C, Berggren PO, Caicedo A. The unique cytoarchitecture of human pancreatic islets has implications for islet cell function. Proc Natl Acad Sci U S A 2006;103:2334–2339
21. Quesada I, Tudurí E, Ripoll C, Nadal A. Physiology of the pancreatic alpha-cell and glucagon secretion: role in glucose homeostasis and diabetes. J Endocrinol 2008;199:5–19
22. Kharouta M, Miller K, Kim A, et al. No mantle formation in rodent islets: the prototype of islet revisited. Diabetes Res Clin Pract 2009;85:252–257
23. Kim A, Miller K, Jo J, Kilimnik G, Wojcik P, Hara M. Islet architecture: a comparative study. Islets 2009;1:129–136
24. Hara M, Wang X, Kawamura T, et al. Transgenic mice with green fluorescent protein-labeled pancreatic beta-cells. Am J Physiol Endocrinol Metab 2003;284:E177–E183
25. Zweifach BW. Quantitative studies of microcirculatory structure and function. I. Analysis of pressure distribution in the terminal vascular bed in cat mesentery. Circ Res 1974;34:843–857
26. Barbu A, Jansson L, Sandberg M, Quach M, Palm F. The use of hydrogen gas clearance for blood flow measurements in single endogenous and transplanted pancreatic islets. Microvasc Res 2015;97:124–129
27. Fowler JL, Lee SS, Wesner ZC, Olehnik SK, Kron SJ, Hara M. Three-dimensional analysis of the human pancreas. Endocrinology 2018;159:1393–1400
28. Steiner DJ, Kim A, Miller K, Hara M. Pancreatic islet plasticity: interspecies comparison of islet architecture and composition. Islets 2010;2:135–145
29. Scott RP, Quaggin SE. Review series: the cell biology of renal filtration. J Cell Biol 2015;209:199–210
30. Rouiller DG, Cirulli V, Halban PA. Uvomorulin mediates calcium-dependent aggregation of islet cells, whereas calcium-independent cell adhesion molecules distinguish between islet cell types. Dev Biol 1991;148:233–242
31. Esni F, Täljedal IB, Perl AK, Cremer H, Christofori G, Semb H. Neural cell adhesion molecule (N-CAM) is required for cell type segregation and normal ultrastructure in pancreatic islets. J Cell Biol 1999;144:325–337
32. Rukstalis JM, Habener JF. Snail2, a mediator of epithelial-mesenchymal transitions, expressed in progenitor cells of the developing endocrine pancreas. Gene Expr Patterns 2007;7:471–479
33. Gouzi M, Kim YH, Katsumoto K, Johansson K, Grapin-Botton A. Neurogenin3 initiates stepwise delamination of differentiating endocrine cells during pancreas development. Dev Dyn 2011;240:589–604
34. Pan FC, Wright C. Pancreas organogenesis: from bud to plexus to gland. Dev Dyn 2011;240:530–565
35. Villasenor A, Cleaver O. Crosstalk between the developing pancreas and its blood vessels: an evolving dialog. Semin Cell Dev Biol 2012;23:685–692
36. Larsen HL, Grapin-Botton A. The molecular and morphogenetic basis of pancreas organogenesis. Semin Cell Dev Biol 2017;66:51–68
37. Augustine P, Gent R, Louise J, et al.; ENDIA Study Group. Pancreas size and exocrine function is decreased in young children with recent-onset type 1 diabetes. Diabet Med. 15 May 2019 [Epub ahead of print]. DOI: 10.1111/dme.13987
38. Campbell-Thompson ML, Kaddis JS, Wasserfall C, et al. The influence of type 1 diabetes on pancreatic weight. Diabetologia 2016;59:217–221
39. Salgado E, Girerd RJ, Horava A. [Insulin as growth factor]. Rev Can Biol 1956;15:187–194 [in French]
40. Logsdon CD. Stimulation of pancreatic acinar cell growth by CCK, epidermal growth factor, and insulin in vitro. Am J Physiol 1986;251:G487–G494
41. Menon RK, Sperling MA. Insulin as a growth factor. Endocrinol Metab Clin North Am 1996;25:633–647
42. Hill DJ, Milner RD. Insulin as a growth factor. Pediatr Res 1985;19:879–886
43. Johnston NR, Mitchell RK, Haythorne E, et al. Beta cell hubs dictate pancreatic islet responses to glucose. Cell Metab 2016;24:389–401
44. Lei CL, Kellard JA, Hara M, Johnson JD, Rodriguez B, Briant LJB. Beta-cell hubs maintain Ca^{2+} oscillations in human and mouse islet simulations. Islets 2018;10:151–167
45. Salem V, Silva LD, Suba K, et al. Leader β-cells coordinate Ca^{2+} dynamics across pancreatic islets in vivo. Nat Metab 2019;1:615–629
46. Krapp A, Knöfler M, Ledermann B, et al. The bHLH protein PTF1-p48 is essential for the formation of the exocrine and the correct spatial organization of the endocrine pancreas. Genes Dev 1998;12:3752–3763
47. Reinert RB, Brissova M, Shostak A, et al. Vascular endothelial growth factor-A and islet vascularization are necessary in developing, but not adult, pancreatic islets. Diabetes 2013;62:4154–4164